Crystal field and energy levels of Pr^{3+} centres in $LiNbO_3$

1998 J. Phys.: Condens. Matter 10 7653

(http://iopscience.iop.org/0953-8984/10/34/018)

J. Phys.: Condens. Matter **10** (1998) 7653–7664. Printed in the UK PII: S0953-8984(98)91081-5

Crystal field and energy levels of Pr^{3+} centres in $LiNbO_3$

J E Muñoz-Santiuste†, A Lorenzo‡, L E Bausá‡ and J García Solé‡

† Departamento de Física, Escuela Politécnica Superior, Universidad Carlos III de Madrid, Butarque 15, Leganés E-28911, Madrid, Spain

‡ Departamento de Física de Materiales C-IV Universidad Autónoma de Madrid, Cantoblanco, E-28049 Madrid, Spain

Received 27 January 1998, in final form 29 May 1998

Abstract. The polarized optical absorption and fluorescence of Pr^{3+} in $LiNbO_3$ crystals have been exhaustively investigated at low temperature in order to obtain and characterize the crystal field energy levels for every multiplet of the system. Up to 51 energy levels have been determined for this ion, and labelled by irreducible representations, E or A, assuming C_3 local symmetry. These energy levels have been used to estimate the crystal field (B_q^k parameters) acting on the Pr^{3+} ion in this host crystal. As the optical spectra present additional structure owing to the presence of four Pr^{3+} centres, laser site selective spectroscopy has been used to determine the Stark sublevels of the $^3H_4$ ground state for each particular centre. Thus, the slight variations of the B_q^k parameters from one centre to another have been investigated and interpreted in terms of different Li^+-off centre positions for Pr^{3+} ions.

1. Introduction

In the search for new compact or integrated solid state active materials, the combination of Pr^{3+} ions and the $LiNbO_3$ matrix appears to be a very promising material that can provide new ranges of emission wavelengths in the visible and near infrared regions.

At present, the interest in studying Pr^{3+}-doped solid-state materials has been renewed owing to the emission spectra of this ion which is extended from the ultraviolet to the near infrared region [1]. Laser action has been reported for different Pr^{3+} crystals such as YAG, $LiYF_4$ and $YAlO_3$, as well as optical amplification in fibres [2–5]. This ion is of additional interest as an active impurity because infrared to blue up-conversion has been demonstrated for a number of Pr^{3+} doped systems [6–8].

On the other hand, the $LiNbO_3$ matrix is a relevant material for integrated optoelectronic devices because of its numerous applications such as optical waveguides and self-frequency doubled solid-state lasers [9, 10].

A number of studies using optical techniques and electron paramagnetic resonance have been devoted to the determination of the site symmetry for different rare earth ions and other types of impurities in $LiNbO_3$ crystals. The authors have recently reported some characteristics of the Pr^{3+}:$LiNbO_3$ system. Room temperature optical absorption and fluorescence bands of Pr^{3+} in $LiNbO_3$ have been investigated in order to determine the absorption and fluorescence channels as well as the excited state dynamics [11]. It has also been demonstrated by means of Rutherford backscattering spectrometry (RBS)/channelling, that Pr^{3+} ions (as well as other trivalent rare earth ions) lie in Li^+ octahedral sites but off centred with respect to the regular Li^+ location [12]. According to that, the local symmetry

0953-8984/98/347653+12$19.50

proposed for Pr^{3+} ions occupying these sites is C_3. Site selective spectroscopy (SSS) experiments also revealed the presence of non-equivalent Pr^{3+} centres [13] responsible for the shape of the low-temperature absorption/emission lines. The presence of these non-equivalent centres was also confirmed by RBS/channelling experiments [14].

In this work systematic research of the polarized low-temperature optical spectra (absorption and luminescence) was carried out from the near infrared to the visible spectral region in order to determine the position and symmetry character of the energy levels of Pr^{3+} in $LiNbO_3$. A crystal field analysis was performed using these experimentally determined energy levels assuming a C_3 local symmetry for the Pr^{3+} ions in $LiNbO_3$, so that the crystal field parameters (B_k^q) were determined. However, provided these parameters are an average value over the different Pr^{3+} centres, SSS was applied in order to determine some energy levels of individual Pr^{3+} centres. This allowed us to investigate the small variation in the crystal field from one centre to another, so that the structure of the Pr^{3+} centres can be advanced within a good agreement between RBS/channelling and spectroscopic results. On the other hand, this approach opens a new way of testing the physical sense of crystal field parameters in terms of slight variations in the local structure.

2. Experimental details

Pr^{3+}-doped $LiNbO_3$ crystals were grown by the Czochralski technique in our laboratory from a congruent melt of grade I Johnson-Matthey powder. Pr_2O_3 was added to the melt in a concentration of 0.2 mol% relative to Nb_2O_5. At the end of the growing process, an electric field was applied to avoid the presence of domains.

Crystals were oriented using x-ray diffraction patterns. Then about 3 mm thick plates were cut and polished with their faces parallel or perpendicular to the ferroelectric c axis.

Polarized absorption spectra were obtained with Cary 17 and Hitachi U3501 spectrophotometers using a Glan–Thompson calcite polarizer. Fluorescence measurements were performed by using either the third harmonic of a pulsed Nd:YAG laser at 355 nm or a continuous Ar^+ laser. For site selective experiments a nitrogen pumped dye laser (perpendicularly polarized to the c axis of $LiNbO_3$, σ configuration) was used. The emitted light was focused on the entrance slit of a SPEX 500M monocromator and detected with a cooled multialkali photomultiplier followed by a photon counting gated system. In the case of continuous excitation, the detector used was a silicon photodiode.

The spectra were taken at low temperature using a closed-cycle helium cryostat, provided with a temperature control, and the measurements were performed at 15 K.

3. Results and discussion

3.1. Determination of energy levels from the optical spectra

The spectra of any rare earth ion in a solid are mostly due to transitions between different states within the $4f^n$ configuration of these ions. In the case of Pr^{3+} ions, the $4f^2$ configuration produces a number of J-states whose degeneracy is partially removed by the action of the matrix crystal field. In our case, assuming C_3 symmetry for the Pr^{3+} ions in the $LiNbO_3$ crystals, any J state of the free ion will split in a number of A and E Stark levels depending on the J-value [15]. The irreducible representation (E or A) associated with each Stark level can be determined by studying the character (electric or magnetic dipole) of the optical transitions between levels. This can be performed experimentally from polarized optical absorption measurements, analysing the so-called α, σ and π polarized spectra.

The α spectrum is taken from samples with the c axis perpendicular to the electric field. The π and σ spectra are taken from samples with the ferroelectric c axis lying along their faces and the electric field of the incident light beam parallel (for π) and perpendicular (for σ) to the c axis. The classification (A or E label) of each Stark energy level from the experimental data can be inferred by taking into account the electric-dipole selection rules for C_3 point-group symmetry as shown elsewhere [15].

It is important to mention that for all the transitions studied in this work, the α and σ spectra had the same shape, while the π polarized absorption spectra were, in each case, significantly different. This fact is in agreement with the transformation properties of the electric-dipole operator; identical axial α and σ-polarized spectra (within a multiplicative factor). Thus, from the α, σ and π spectra it is possible to ascertain that transitions between the Stark levels have primarily electric-dipole character.

Figures 1(a)–(d) display, as an example, the absorption spectra from the $^3H_4$ ground state to the $^3P_{2,1,0}$, $^1D_2$, $^3F_{4,3,2}$ and $^3H_6$ excited states for the σ and π polarizations, at low temperature. Table 1 lists all the experimentally determined energy levels and their symmetry assignment (when possible) for each Stark level.

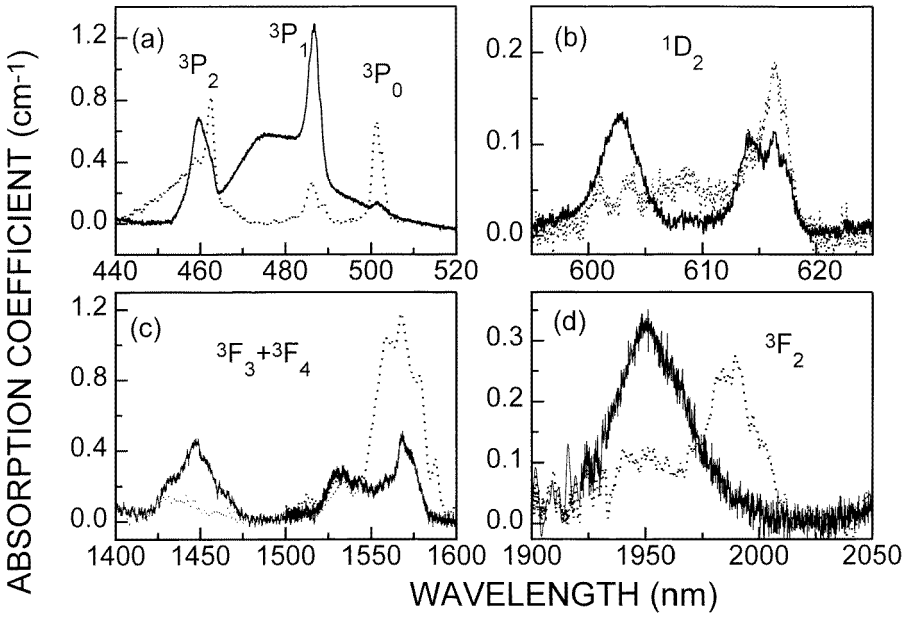

Figure 1. Polarized absorption spectra of Pr^{3+} in $LiNbO_3$ at 15 K. Full curve, π configuration; dotted curve, σ configuration.

An important goal is the determination of the polarization character (E or A) of the low-energy Stark level of the $^3H_4$ ground state ($^3H_4(0)$ fundamental level) which is referred to as the origin of the energy scale. Taking advantage of the non-degeneration of the $^3P_0$ excited state, the single Stark level for this state can be identified as an A type level in C_3 crystal field symmetry. Thus, the absorption band associated with the $^3H_4(0) \rightarrow {}^3P_0$ transition permit, using the selection rules, obtaining the character of the fundamental level.

Figure 1(a) includes the above mentioned absorption transition for the σ and π polarization. As observed, the $^3H_4(0) \rightarrow {}^3P_0$ transition is clearly σ polarized. Thus, from the electric-dipole selection rules it is possible to conclude that the fundamental level

Table 1. Experimental and calculated energy level positions (cm^{-1}) and irreducible representation label for Pr^{3+} ions in $LiNbO_3$. The Hamiltonian parameters used to obtain the calculated values are included.

	Experimental			Calculated			
	Absorption	Emission		C_{3v}		C_3	
$^1S_0$				46 913	A	46 907	A
$^3P_2$	21 758		E	21 757	E	21 762	E
	21 683		E	21 742	A	21 740	A
	21 609		A	21 649	E	21 641	E
$^1I_6$				21 566	E	21 531	A
				21 509	A	21 523	A
				21 498	A	21 522	E
				21 497	E	21 488	E
				21 282	A	21 266	A
				21 263	A	21 246	A
				21 052	E	21 058	E
				20 874	E	20 899	E
				20 812	A	20 840	A
$^3P_1$	20 597		E1	20 541	E	20 538	E
	20 559		E2				
	20 542		E3				
	20 487		E4				
	20 445		A	20 391	A	20 391	A
$^3P_0$	19 960		A1	19 943	A	19 943	A
	19 940		A2				
	19 900		A3				
	19 869		A4				
$^1D_2$	16 584			16 631	E	16 613	E
	16 420			16 339	A	16 370	A
	16 260			16 249	E	16 250	E
$^1G_4$	10 200	10 199	E	10 139	E	10 158	E
	10 129	10 121	E	10 115	A	10 135	A
	9984	9990	A	10 030	E	10 029	E
	9862	9860	A	9837	E	9814	E
	9751	9745	E	9792	A	9777	A
	9474	9485	A	9568	A	9569	A
$^3F_3 + {}^3F_4$		6953		6923	A	6916	A
		6872		6910	E	6900	E
		6788		6802	E	6802	E
		6718		6742	E	6750	E
		6689		6674	A	6686	A
		6660		6604	A	6612	A
	6506	6506	E	6440	A	6445	E
	6468	6468	A	6438	E	6438	A
	6398	6398	A	6384	A	6366	A
	6365	6365	E	6357	E	6341	E
	6321	6321	A	6328	A	6337	A
$^3F_2$	5196		A1	5116	A	5108	A
	5083	5096	A2				
	5025		E1	5034	E	5044	E
	5015	5020	E2				
	4941	4941	E	4984	E	4993	E

Table 1. Continued.

	Experimental		Calculated			
	Absorption	Emission	C_{3v}		C_3	
$^3H_6$		4803	4737	A	4745	A
		4663	4731	A	4732	A
		4506	4503	E	4515	E
		4428	4420	A	4427	A
		4382	4410	E	4398	E
		4263	4243	E	4255	E
		4231	4233	A	4211	A
		4202	4168	E	4176	E
		4148	4144	A	4079	A
$^3H_5$		2543	2555	E	2547	E
		2297	2326	E	2328	E
		2171	2296	A	2295	A
		2148	2168	E	2174	E
		2127	2136	A	2162	A
		2120	2123	E	2121	E
		2098	2102	A	2092	A
$^3H_4$		503	489	E	483	E
(average)		384	283	A	280	A
		145	109	E	126	A
		94	85	A	95	E
		31	37	A	38	A
		0 E	16	E	9	E

Free ion and crystal field parameters		
	C_{3v}	C_3
E_1	4573	4574
E_2	21.2	21.1
E_3	449	449
ξ	776	773
α	26.9	21.8
β	−1060	−1023
γ	1479	1462
M_0	4.1	3.9
P_2	−127	−84
B_2^0	−578	−563
B_4^0	−1310	−1128
B_4^3	657	−647
B_6^0	−339	−399
B_6^3	−241	−398
S_6^3		631
B_6^6	−386	−316
S_6^6		−26
rms	40	40

is E type. The identification of the Stark levels of the excited states has been carried out taking this into account.

The presence of thermalized absorption bands departing from excited Stark levels belonging to the $^3H_4$ ground state has been disregarded at the temperatures considered in this work (15 K). The variations of the absorption spectra as the temperature increases confirm this point and, as will be shown later, the two first excited levels are located at 31 cm^{-1} and 91 cm^{-1} respectively above the fundamental one (0 cm^{-1}).

To determine the Stark levels of the $^3H_{4,5,6}$ multiplet, fluorescence spectra were also taken and transitions terminating in these states are included in figure 2 ((a)–(c)). In addition, the emissions to other states, such as $^3F_{2,3,4}$ and $^1G_4$, were also obtained (figures 2(d)–(f)) and used to confirm the positions of the energy levels obtained from the absorption spectra.

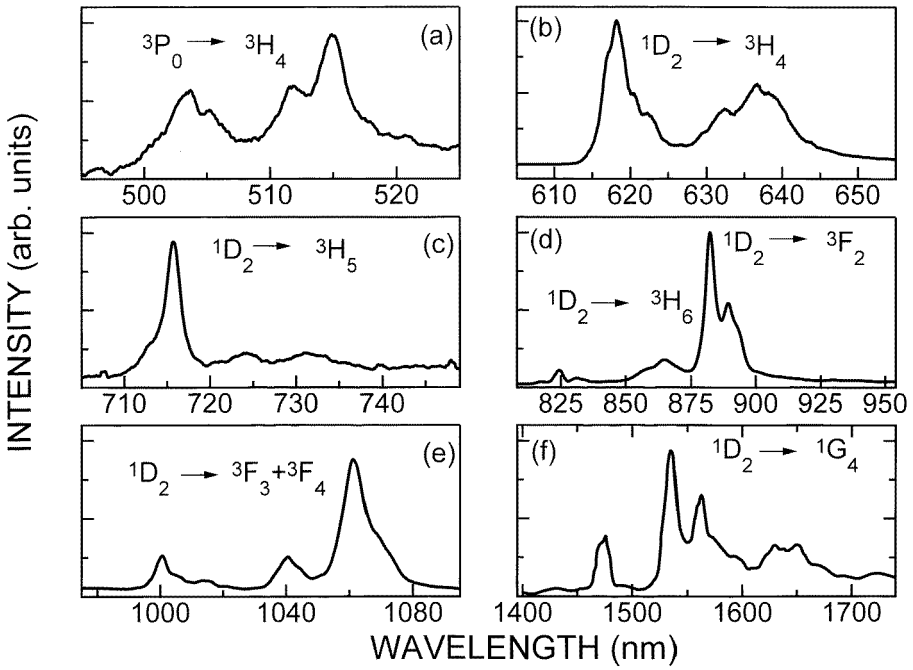

Figure 2. Emission spectra of Pr^{3+} in $LiNbO_3$ at 15 K.

The energy levels obtained from all these optical spectra are included in table 1. A total number of 51 levels have been identified and conveniently labelled by irreducible representations E or A.

In some of the absorption spectra we can observe a number of bands which is higher than that predicted by the group theory for a C_3 symmetry and a fixed J value. In $LiNbO_3$ this excess of lines has been attributed to multicentres, i.e. Pr^{3+} ions in Li^+ octahedral sites with slightly different local environments. Because the capability to resolve the transitions associated with centres depends on the sensibility of each particular transition to crystal field changes, in most of the absorption transitions only a strong broadening of bands is observed. Only a few transitions clearly show the multicentre structure inside the absorption band (namely $^3P_0$, $^3P_1$ and partially $^1D_2$). Those peaks that are clearly related to the same absorption transition for several centres are included in table 1 and labelled by adding a numerical suffix to the corresponding representation label.

As a relevant example, figure 3(a) displays the σ-type $^3H_4(0) \rightarrow {}^3P_0$ absorption band which should consist of a single band but exhibits a fourfold structure corresponding to four non-equivalent Pr^{3+} optical centres. The presence of these non-equivalent Pr^{3+} centres was confirmed by SSS [13] and RBS/channelling spectra [12, 13, 16]. These centres were explained as a result of four different off-centred positions along the *c* axis scattered in the range from ∼0.35 Å (centre IV), to ∼0.45 Å (centre I) as is shown in figure 4 [14]. Additionally, a systematic analysis of the SSS spectra allowed us to construct an experimentally determined energy diagram of the $^3H_4$ state for each of the above mentioned Pr^{3+} different centres. This diagram is shown in figure 3(b) taking the energy position of the $^3P_0$ level as an energy reference for each centre. The Pr^{3+} centres have been labelled as I, II, III and IV in order of decreasing $^3H_4$ splitting. This diagram will be used later on to obtain a particular set of crystal field parameters for each different Pr^{3+} centre.

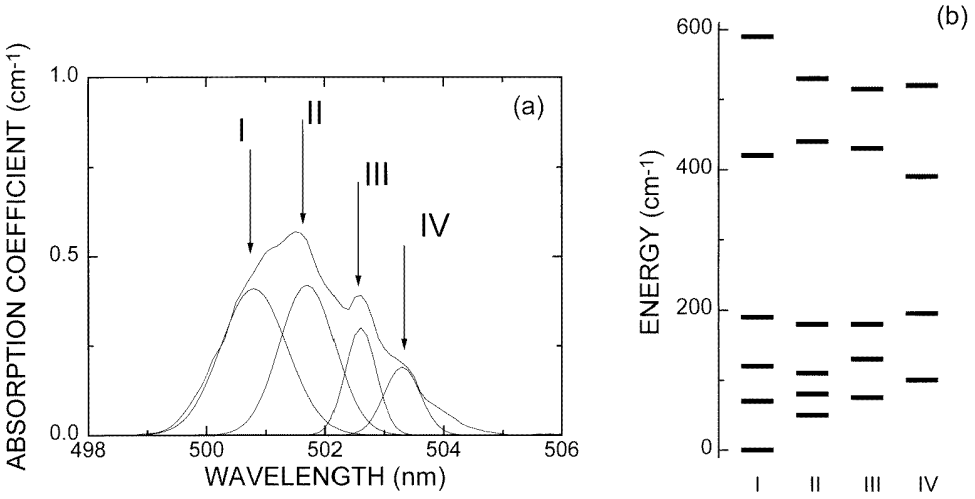

Figure 3. (a) $^3H_4(0) \rightarrow {}^3P_0$ absorption transition, showing the presence of four Pr^{3+} centres, denoted by I, II, III and IV (15 K). (b) Energy level diagram for the $^3H_4$ state of each Pr^{3+} centre. After [13].

3.2. Crystal field analysis

For an energy level calculation of lanthanide ions in solids, we assume that the electronic states are only slightly perturbed by the electric potential of their environment and so the crystal field Hamiltonian, H_{CF}, can be treated as a small perturbation of the free ion Hamiltonian, H_0. Thus the total Hamiltonian is

$$H = H_0 + H_{CF}.$$

The semiempirical strategy to perform the calculation of energy levels is to take advantage of the fact that the various interactions contributing to the Hamiltonian can be factorized in their angular contributions, which can be exactly calculated, and their radial contributions which are treated as adjustable parameters.

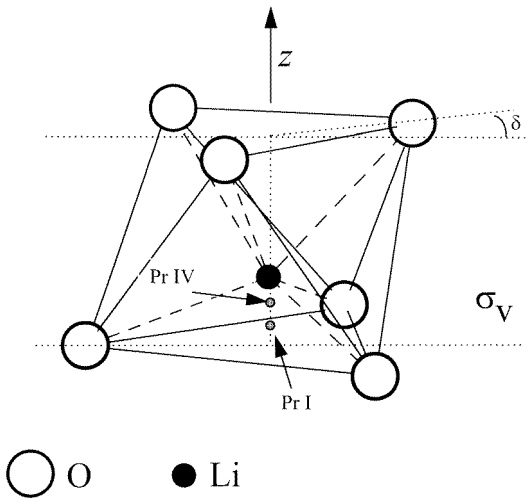

Figure 4. Li^{+} octahedron in $LiNbO_3$. The location of two Pr^{3+} centres (I and IV) is indicated.

For the $4f^2$ configuration, the free ion Hamiltonian including the electrostatic, spin–orbit, trees and magnetic interactions is

$$H_0 = \sum_k E_k e^k + \xi A_{SO} + \alpha L(L+1) + \beta G(G_2) + \gamma G(R_7) + \sum_k P_k p^k + \sum_k M_k m^k$$

where e^k and A_{SO} are the angular contributions of the electrostatic term and spin–orbit interaction, L is the total orbital angular momentum, $G(G_2)$ and $G(R_7)$ are the eigenvalues of Casimir's operators G_2 and R_7, and p^k, m^k deal with the angular contributions of the magnetic interactions. The values of these parameters for the Pr^{3+} ion can be calculated from previously tabulated data [17–21]. The remaining factors correspond to the radial part and are treated as adjustable parameters. To achieve the calculation reported below, the parameters M_k and P_k are constricted to their ratios $M_2/M_0 = 0.56$, $M_4/M_0 = 0.38$ and $P_4/P_2 = 0.75$, $P_6/P_2 = 0.50$ [19], in order to obtain a more reduced set of parameters (nine free ion parameters, namely E_1, E_2, E_3, ξ, α, β, γ, M_0, and P_2 and the average energy of the whole 4f configuration).

The crystal field Hamiltonian, H_{CF}, is given by

$$H_{CF} = \sum_{k=0}^{\leqslant 6} \sum_{q \geqslant -k}^{\leqslant k} B_k^q [C_q^{(k)} + (-1)^q C_{-q}^{(k)}] + \mathrm{i} S_k^q [C_q^{(k)} - (-1)^q C_{-q}^{(k)}]$$

where $C_q^{(k)}$ are the spherical tensor operators whereas B_k^q, S_k^q are the real and imaginary parts of the adjustable crystal field parameters. The spherical tensors can be obtained from the tabulated values of the reduced matrix elements [20] and 6j-symbols [21]. The number of non-zero crystal field parameters depends on the point symmetry at the site of the lanthanide ion. Rare earth ions occupy octahedral sites in the $LiNbO_3$ matrix, with C_3 (near C_{3v}) symmetry.

In trigonal C_3 symmetry, H_{CF} involves nine non-zero parameters (six real parameters, B_2^0, B_4^0, B_4^3, B_6^0, B_6^3 and B_6^6, and three complex ones, S_4^3, S_6^3 and S_6^6). From algebraic considerations for a C_3 symmetry crystal field Hamiltonian, it follows that different combinations of the crystal field parameters can lead to the same energy level values [22]. To obtain a standard group of crystal field parameters it is necessary to make some restrictions

by selecting a special axis system. The S_4^3 parameter can be selected to be zero by means of a rotation about the Oz axis (the c axis). This selection ($S_4^3 = 0$) permits to obtain a standardized set of parameters to be obtained for C_3 symmetry [22].

The octahedral sites in the $LiNbO_3$ structure has C_3 (near C_{3v}) symmetry. The departure from C_{3v} symmetry is measured by the angle δ of the rotation of the upper (or equivalently the lower) triangle of oxygens from the σ_v plane (see figure 4) [23]. Since this angle is not large ($\delta \sim 3.82$ degrees for Li^+ octahedrons) [24, 25] the approximated C_{3v} symmetry appears as a good starting point to perform the calculations. In C_{3v} symmetry H_{CF} has only real parameters when a coordinate system with Oz axis parallel to the trigonal axis (c axis) and Oy axis parallel to a σ_v plane is selected [22].

The free Ion and crystal field parameters were obtained by diagonalizing the complete Hamiltonian for the Pr^{3+} ion including full J mixing and refining of parameters by using least squares fits that minimize the differences between experimental and calculated energy level positions. From the previous considerations a two step method was followed to fit the experimentally determined energy levels. First an approximated C_{3v} symmetry was used. This approximation greatly simplifies the energy level fitting procedure because only real parameters are included in the calculations. Secondly, the actual C_3 symmetry is considered, including the imaginary parameters in the fitting procedure. The complete Hamiltonian used in the least squares fitting procedure for Pr^{3+} levels has nine free ion parameters and six or eight crystal field parameters for C_{3v} or C_3 symmetry group (selecting $S_4^3 = 0$) respectively. We used the free ion parameters determined by Carnall [26] as initial values, and the crystal field ones determined by Morrison [26, 27] for trivalent rare earth ions in oxygen ligand trigonal symmetry.

The parameters obtained in the least squares fit for both C_{3v} and C_3 symmetries and the calculated energy levels are included in table 1 together with the experimental data. As can be shown in this table, the fitting is not improved, within the error, when using C_3 (actual) symmetry instead of C_{3v} symmetry (approximated).

The root-mean-square deviation between calculated and experimental levels ($\sim$40 cm^{-1}) is very high. However, this is a typical feature of the Pr^{3+} ion as previous studies have shown [28], and can be attributed to two reasons. First, the absence of experimental values for the energy positions of components of the $^1S_0$ and $^1I_6$ terms, which makes the appropriate fit of the free ion parameters difficult. Second, and more important, the already mentioned presence of at least four different Pr^{3+} centres in this system. In this sense, the set of crystal field parameters in table 1 should be understood as an averaged value over the different Pr^{3+} centres in the system.

3.3. Energy levels of the Pr^{3+} centres

Once the crystal field parameter (as average values) was determined for the Pr^{3+} ions in $LiNbO_3$, a crystal field analysis was performed using the experimentally obtained energy levels of each particular centre.

Taking advantage of the good resolution obtained for the $^3H_4$ ground state (see figure 3(b)), we can obtain a crystal field parameter set for each centre using the energy levels of this state. From this calculation we obtain a rough estimation of the crystal field parameters that can be associated with each optical centre. From the former results, the simplified C_{3v} symmetry is used to reduce the number of crystal field parameters. A weighted function is used in this restricted calculation to force the fitting to the experimental $^3H_4$ levels. Table 2 lists the set of parameters obtained for each centre.

The Pr^{3+} centres can be identified by the amount of splitting in the $^3H_4$ state. Figure 5

Table 2. Crystal field parameters obtained for each centre.

	Pr^{3+} centre			
	I	II	III	IV
B_2^0	−673	−530	−505	−533
B_4^0	−1295	−953	−901	−1027
B_4^3	775	874	879	631
B_6^0	−881	−724	−677	−618
B_6^3	−296	−326	−164	−162
B_6^6	−754	−818	−310	−233

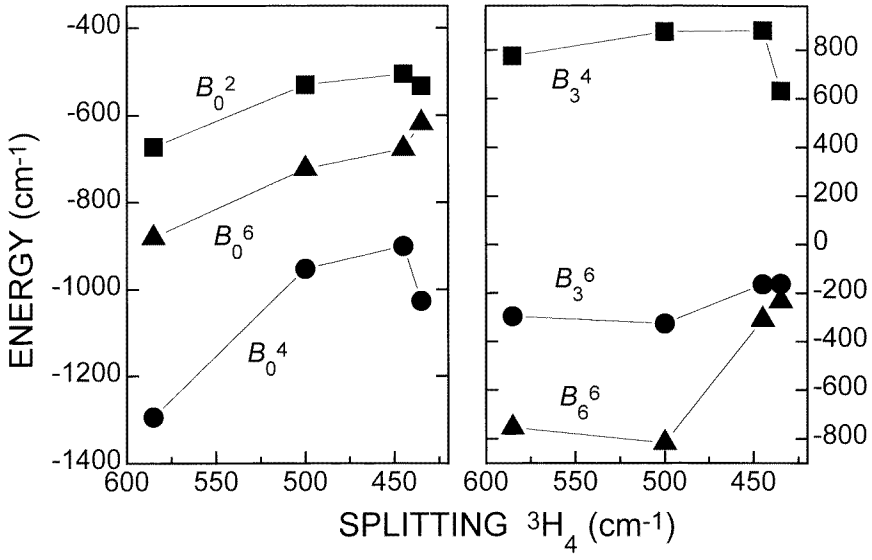

Figure 5. B_k^q parameters against $^3H_4$ splitting for the different Pr^{3+} centres. Full curves are only to guide the eyes.

shows the B_k^q parameters as a function of the $^3H_4$ splitting for each particular centre. An inspection of this figure reveals how the crystal field parameters show a relatively smooth variation among the centres. This fact is expected because the differences between centres are due to the small changes in the environment of the Pr^{3+} ion.

Let us now comment on the observed changes. The variation obtained in the B_2^0 axial parameter can be explained if we take into account the previously proposed structure for the different Pr^{3+} centres by RBS/channelling [12, 14]. As formerly mentioned, these centres would correspond to different off-centre displacements of the Pr^{3+} ions from the Li^+ sites towards the nearest oxygen triangle (see figure 4). Thus, it is expected that the B_2^0 axial parameter increases with the displacement from the Li^+ site position (or from the centre of the Li^+ octahedron). This can be intuitively deduced from figure 4, the larger off-centre displacement, the higher B_2^0 value and the larger the $^3H_4$ splitting. According to this, the centre I ($^3H_4$ splitting $\sim$600 cm^{-1}) would be the most off-centred in the Li octahedron, while

the III and IV centres would appear less displaced. In fact, according to the RBS/channelling results [14] it could be concluded that the centre I would be shifted by about 0.45 Å from the regular Li^+ position, while those for III and IV should be located at a very close position, about 0.35 Å from the Li^+ site. Obviously, these non-equivalent off-centre positions of Pr^{3+} (or Pr^{3+} centres) must also affect the other B_k^q parameters, as experimentally observed in figure 5.

As previous works have pointed out [29] the values of the fourth rank parameters ($k = 4$) are strongly increased by covalence effects in the chemical bonds. Variation in the covalence of the Pr–O bonds can be a consequence of the different overlapping between the wavefunctions of Pr ions and those of the oxygen ligands due to the displacement of the Pr ions along the c axis. This fact is reflected by the behaviour of the B_4^0 parameter. Additionally, the similar behaviour of all the B_k^0 parameters points to a common origin and we can assume that Pr^{3+} displacements along the ferroelectric c axis is the main factor responsible for the variation of all these parameters. Moreover, taking into account the expected relaxation of the oxygen octahedron to compensate for the effect of axial displacement of the Pr^{3+} ion, the relatively small variation obtained for the B_4^3 parameter can also be understood.

The physical meaning of the sixth rank parameters ($k = 6$), associated with short distance interactions, cannot be analysed. The B_6^3 and B_6^6 parameters must be greatly undetermined by the selection of the simplified C_{3v} symmetry ($S_6^3 = S_6^6 = 0$). Moreover, the B_6^0 parameter is strongly overestimated (compared with the value obtained in the calculation included in table 1) indicating that more than the $^3H_4$ levels must be included in the calculation to obtain accurate values of this parameter.

In any case, these types of studies present a straightforward way to analyse the physical meaning of the B_k^q crystal field parameters. In fact, the small changes the B_k^q parameters that are observed from one centre to another, should be interpreted as slight deviations in the environment of the tested doping ion (Pr^{3+} in this case). Therefore, the effects due to changes in the coordination number, local symmetry, type of ligand ions and so on, are avoided and the dependence of the B_k^q parameters on ligand distances could be faced.

4. Conclusion

The majority (51) of the Stark energy levels of Pr^{3+} in $LiNbO_3$ has been determined and labelled by means of the irreducible representations, E or A, in good agreement with C_3 local symmetry (Li^+ sites). These experimentally determined energy levels have been used to determine the total Hamiltonian (free ion and crystal field parameters) of the Pr^{3+} ion in this matrix. Finally, the multicentre structure observed on the optical spectra has been studied. Site selective spectroscopy has been used to obtain the energy levels of the $^3H_4$ ground state for each of the four detected Pr^{3+} centres. These energy levels have been used to determine the B_k^q crystal field parameters for each particular Pr^{3+} centre. The slight variations in the crystal field among the different centres have been investigated. The obtained results are in good agreement with the presence of different off-centre positions for Pr^{3+} ions inside the Li^+ octahedron.

Acknowledgments

This work has been supported by the CICYT of the Spanish Government under project MAT 95-152.

References

[1] Malinowski M, Joubert M F and Jaquier B 1993 *Phys. Status Solidi* a **140** k49
[2] Wolinski W, Wolski R, Malinowski M and Mierczyk Z 1992 *Proc. 10th Inter. Congr. Laser'91* (Munich: Springer) p 611
[3] Esterowitz L, Allen R, Kruer M, Bartoli F, Goldberg L S, Jensen H P, Linz A and Nicolaik V O 1977 *J. Appl. Phys.* **48** 650
[4] Belckmnan A, Heine F, Meyn J P, Petermann K and Huber G 1993 *OSA Proc. Adv. Solid State Lasers* ATuB1, 164
[5] Carter S F, Szebesta D, Davey S T, Wyatt R, Brieley M C and France P W 1991 *Electron. Lett.* **27** 628
[6] Malinowski M 1989 *J. Phys.: Condens. Matter* **1** 4673
[7] Malinowski M and Strek W 1987 *J. Phys. C: Solid State Phys.* **20** 2595
[8] Malinowski M, Joubert M F and Jaquier B 1994 *J. Lumin.* **60&61** 179
[9] Cordova-Plaza A, Digonnet M J and Shaw H J 1987 *IEEE J. Quantum Electron.* **23** 262
[10] Lallier E, Pocholle J P, Papuchon M, de Micheli M, Li M J, He Q, Ostrowski D P, Crezes-Besnet G and Pelletier E 1990 *Opt. Lett.* **15** 682
[11] Lorenzo A, Bausá L E and García Solé J 1995 *Phys. Rev.* B **51** 16 643
[12] Lorenzo A, Jaffrezic H, Roux B, Boulon G and García Solé J 1995 *Appl. Phys. Lett.* **67** 3735
[13] Lorenzo A, Jaffrezic H, Roux B, Boulon G, Bausá L E and García Solé J 1995 *Phys. Rev.* B **52** 6278
[14] Lorenzo A, Loro H, Muñoz-Santiuste J E, Terrile M C, Boulon G, Bausá L E and García Solé J 1997 *Opt. Mat.* **8** 55
[15] Henderson B and Imbusch G F 1989 *Optical Spectroscopy of Inorganic Solids* (Oxford: Clarendon)
[16] Lorenzo A, Bausá L E, Voda M and García Solé J 1994 *J. Physique* IV **C-4** 381
[17] Crosswhite H M, Crosswhite H, Kaseta F W and Sarup R 1976 *J. Chem. Phys.* **64** 1981
[18] Wybourne B G 1966 *Spectroscopic Properties of Rare Earths* (New York: Interscience)
[19] Judd B R and Crosswhite H 1984 *J. Opt. Soc. Am.* B **1** 255
[20] Nielson C W and Koster G F 1964 *Spectroscopic Coefficients for p^n, d^n and f^n Configurations* (Cambridge, MA: MIT Press)
[21] Computer program MATHEMATICA, version 2.2, 1993 Wolfram Research Inc.
[22] Rudowicz C 1986 *Chem. Phys.* **102** 437
[23] Glass A M 1969 *J. Chem. Phys.* **50** 1501
[24] Abraham S C, Reddy J M and Bernstein J L 1966 *J. Chem. Phys. Solids* **27** 997
[25] Abraham S C and Marsh P 1986 *Acta Crystallogr.* B **42** 61
[26] Carnall W T, Goodman G L, Rajnak K and Rana R S 1989 *J. Chem. Phys.* **90** 3443
[27] Morrison C A and Leavitt R P 1981 *J. Chem. Phys.* **74** 25
[28] Morrison C A, Leavitt R P and Wortman D E 1980 *J. Chem. Phys.* **73** 2580
[29] Antic-Fidancev E, Lemaitre-Blaise M and Caro P 1987 *New J. Chem.* **11** 467